Supplement of Atmos. Chem. Phys., 14, 4661–4678, 2014
http://www.atmos-chem-phys.net/acp-14-4661-2014/
doi:10.5194/acp-14-4661-2014-supplement

Atmospheric Chemistry and Physics Open Access

Supplement of

Secondary organic aerosol formation exceeds primary particulate matter emissions for light-duty gasoline vehicles

T. D. Gordon et al.

Correspondence to: A. Robinson (alr@andrew.cmu.edu)

Supplementary Information

Table S.1 Specifications of all 15 different vehicles tested in the chamber are found in the left half of the table. Gas- and particle-phase concentrations in the chamber (CO measured in CVS) at t=0 h and other key experimental conditions for all 29 chamber experiments are found in the right half. Most vehicles were tested more than once. Primary emission factors and SOA production are shown in Table S.6.

	test date	CARB test ID	expt ID	model year	vehicle class	engine size (L)	emission standard	mileage	UC driving cycle	VOC/ NOx	seed	mpg	POA ($\mu g/m^3$)	BC ($\mu g/m^3$)	CO (g/kg)	ΔCO_2 (ppm)	NO (ppb)	NO_2 (ppb)	d-butanol (ppm)	propene (ppm)	NMOG (ppmC)	OH exposure
Pre-LEV	2/14/12	1032442	PreLEV-1.1	1987	PC	4.1	Tier I	197,631	Cold	3.32	N	14.6	2.0	2.7	209.5	99	1095	0	0.06	0.13	1.82	6.8E+06
	2/10/12	1032440	PreLEV-2.1	1988	PC	1.6	Tier I	224,758	Cold	4.31	N	24.1	9.2	5.7	332.3	206	1558	0	0.06	0.00	8.20	5.5E+06
	2/13/12	1032444	PreLEV-2.2						Cold	4.62	N	23.8	3.9	2.4	328.2	99	1095	0	0.06	0.00	3.20	6.7E+06
	1/31/12	1032303	PreLEV-3.2						Cold	3.03	Y	13.1	22.7	0.8	72.1	452	1558	0	0.06	1.00	n/a	7.7E+06
	2/1/12	1032389	PreLEV-3.3	1990	M3	5.0	Tier I	58,617	Cold	3.02	Y	12.9	19.0	0.8	73.1	407	1375	0	0.06	0.80	2.61	7.7E+06
	2/8/12	1032426	PreLEV-3.4						Hot	3.08	Y	13.1	0.0	0.8	49.6	423	1117	0	0.06	0.60	2.91	7.0E+06
LEV I	5/26/10	1027859	LEV1-1.5	1996	PC	2.7	Tier I	51,826	Cold	3.80	N	20.4	0.3	0.3	19.8	335	456	0	0.00	0.50	0.31	8.8E+06
	1/17/12	1032302	LEV1-2.1						Cold	3.17	Y	19.3	0.8	0.7	17.9	318	9	651	0.06	0.67	2.00	9.4E+06
	1/18/12	1032304	LEV1-2.2	1997	PC	3.0	LEV	130,485	Cold	3.91	Y	19.2	0.5	0.9	22.6	245	203	68	0.12	0.20	0.97	8.9E+06
	2/15/12	1032473	LEV1-2.3						Hot	3.12	Y	19.1	0.5	0.7	10.0	264	183	76	0.06	0.27	1.06	7.5E+06
	1/25/12	1032346	LEV1-3.2	1998	PC	3.0	LEV	90,638	Cold	3.16	Y	18.8	1.1	0.7	24.6	288	690	149	0.06	0.73	1.81	8.1E+06
	1/26/12	1032362	LEV1-3.4						Cold	3.20	Y	18.3	0.9	0.5	28.4	269	364	50	0.06	0.33	1.36	7.7E+06
	2/6/12	1032393	LEV1-4.1	1999	PC	2.0	TLEV	118,294	Cold	2.93	Y	23.6	0.8	0.6	45.3	235	400	32	0.06	0.53	1.24	8.0E+06
	6/3/10	1027904	LEV1-5.2	2000	PC	2.2	LEV I, ULEV	104,446	Cold	3.37	N	23.0	2.7	0.5	14.8	252	170	182	0.00	0.35	0.15	1.1E+07
	5/28/10	1027881	LEV1-6.1						Cold	3.48	N	17.1	0.9	8.3	162.6	119	1149	218	0.00	0.75	2.63	3.9E+06
	6/1/10	1027917	LEV1-6.2	2003	PC	3.5	LEV I, NLEV	110,445	Cold	3.47	N	16.5	2.4	5.4	157.5	108	855	172	0.00	0.70	1.75	6.9E+06
	6/2/10	1027918	LEV1-6.3						Cold	0.25	N	18.3	0.4	3.2	155.5	91	1570	0	0.00	0.00	1.73	n/a
LEV II	5/27/10	1027865	LEV2-1.2	2007	M3	3.9	LEV II	29,433	Cold	3.43	N	16.6	0.7	3.6	17.9	416	93	221	0.00	0.25	0.16	5.7E+06
	6/9/10	1027967	LEV2-1.6						Cold	3.28	N	16.4	0.6	4.9	21.2	317	61	168	0.00	0.20	0.12	7.5E+06
	6/15/10	1028022	LEV2-2.1	2008	LDT	4.2	LEV II	43,378	Cold	4.18	N	15.4	0.6	7.9	7.8	388	83	119	0.00	0.25	0.14	1.2E+07
	1/12/12	1032268	LEV2-3.1						Cold	3.24	Y	19.7	0.4	1.7	7.1	165	138	74	0.06	0.13	0.82	1.1E+07
	1/13/12	1032283	LEV2-3.2	2008	PC	3.5	LEV II	35,786	Cold	3.31	Y	19.6	0.7	3.1	9.1	162	220	155	0.06	0.51	1.60	1.0E+07
	1/27/12	1032360	LEV2-3.3						Hot	2.97	Y	20.4	0.6	4.0	2.1	265	146	144	0.06	0.20	0.80	8.3E+06
	1/30/12	1032359	LEV2-3.4						Hot	3.23	Y	21.3	1.0	4.6	1.2	290	137	174	0.06	0.27	0.80	1.1E+07
	6/10/10	1027971	LEV2-4.2	2010	T2	3.6	ULEV; Tier II	18,236	Cold	4.06	N	15.8	0.8	11.4	6.3	336	23	166	0.06	0.06	0.59	1.1E+07
	1/23/12	1032342	LEV2-5.1	2011	PC	2.0	ULEV	10,911	Cold	3.12	Y	21.1	0.7	4.9	21.4	224	301	267	0.06	0.60	0.89	1.0E+07
	1/24/12	1032351	LEV2-5.2						Cold	3.19	Y	22.3	0.9	6.2	15.0	237	304	268	0.06	0.47	1.20	1.4E+07
	1/19/12	1032309	LEV2-6.2	2011	PC	3.6	LEV II, ULEV	29,249	Cold	3.29	Y	15.8	0.6	0.4	12.0	315	96	117	0.06	0.13	1.92	1.2E+07
	1/20/12	1032321	LEV2-6.3						Cold	3.29	Y	15.9	0.6	0.5	9.2	298	9	239	0.06	0.13	0.66	1.8E+07

Table S.2 Fuel analysis of gasoline used in all LDGV experiments.

ethanol (wt%)	oxygen (mass%)	benzene (vol%)	aromatics (vol%)	olefins (vol%)	olefins/ naphthalenes (mass%)	poly- naphthalenes (mass%)	RVP (psi)	T_{10} (°F)	T_{50} (°F)	T_{90} (°F)	sulfur (ppm)	density (g/ml)
ASTM 4815, GC/FID		ASTM D5580, GC/FID		ASTM 6550 SFC			ASTM D5191	ASTM D86			ASTM 5453 ANTEK	ASTM D4052
6.08	2.11	0.56	23.8	5.20	12.38	0.08	6.8	135	212	313	8.80	0.7410

Table S.3 Chemical analysis of gasoline used in all LDGV experiments, listed as mass percentages per carbon number.

	C_4	C_5	C_6	C_7	C_8	C_9	C_{10}	C_{11+}
paraffins	0.69	9.12	11.45	11.62	12.8	3.05	1.27	2.29
aromatics	--	--	0.66	6.12	10.17	8.32	2.14	0.9
cyclic olefins	--	0.08	0.26	0.19	0.06	0.01	--	--
olefins/naph-thalenes	12.38							
polynaph-thalenes	0.22							
MTBE	6.2							
TOTAL (mass%)	**100% = 84.97% C + 13.91% H + 1.12% O**							

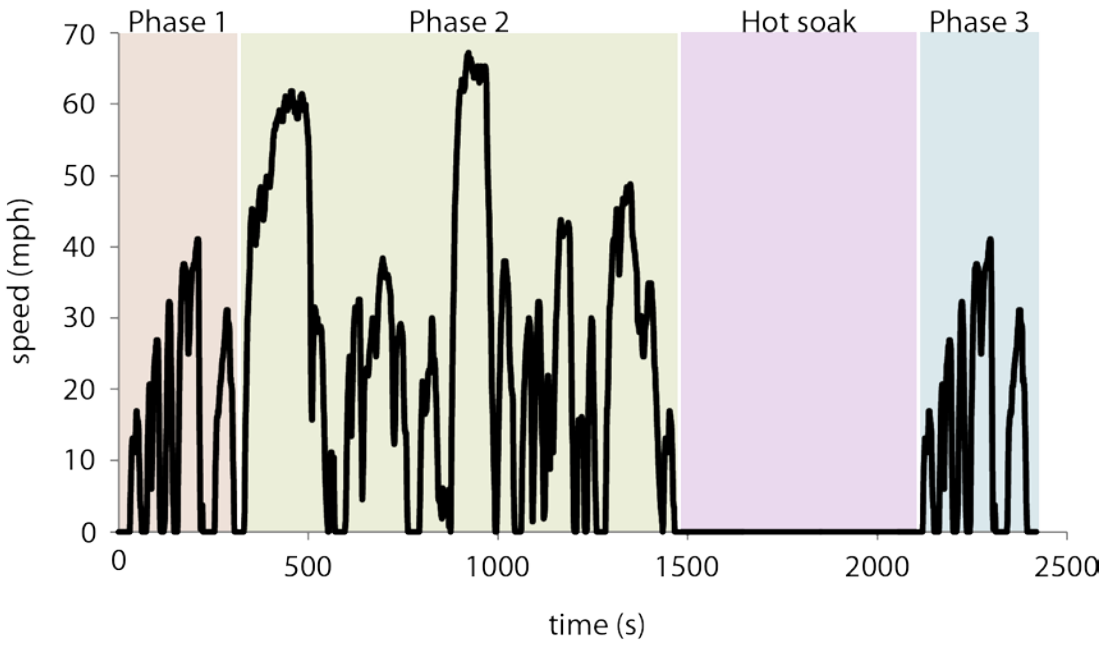

Figure S.1 All vehicles were operated on a chassis dynamometer according to the Unified Cycle (UC), which consists of three phases, simulating urban stop-and-go driving conditions.

Table S.4 Comparison of the unified cycle (UC) and FTP-75 cycle. The UC, used in this study, is a more aggressive cycle than the FTP.

driving cycle	duration (s)	distance (mi)	avg speed (mph)	max speed (mph)	max accel (mph/s)	stops/ mile	% idle	notes
UC	2035	9.8	24.6	67	6.15	1.52	16.4	600 s hot soak not included in avg speed or % idle values
FTP-75	1377	7.5	19.6	56.7	3.31	2.41	19	for comparison only; not used in this study

http://www.dieselnet.com/standards/cycles/hhddt.php
http://www.arb.ca.gov/msei/onroad/briefs/Publication3.pdf

Quantifying SOA Production

To quantify SOA production in the smog chamber we corrected the measured concentrations of suspended particles for (a) the loss of organic particles and vapors to the chamber walls, (b) the increase in the particle loss rate for experiments in which nucleation occurs, and (c) the lower particle detection efficiency by the aerosol mass spectrometer (AMS) for particles smaller than about 60 nm. Wall-loss corrections (1) are important in every experiment, whereas corrections for (b) and (c) are significant only for experiments when photo-oxidation induced nucleation, causing chamber concentrations to be dominated by smaller particles. Correction (a) is described below; corrections (b) and (c) are described in the SI.

Organic particles and vapors are lost to the chamber walls as a function of time, and total OA is the sum of the measured (via the AMS) suspended mass plus the mass of organics on the chamber walls

$$OA_{total,t} = OA_{sus,t} + OA_{wall,t} \quad (1)$$

Organics may be lost to the chamber walls as particles or vapors. Loss of organic particles is treated as a first-order process [31] with a rate constant determined from the decay of BC measured by the aethalometer

$$C(t) = C_0 e^{kt}$$

where C is the BC concentration at time t, C_o is the initial BC concentration and k is the wall-loss rate constant. The wall-loss rate constant depends on the size and composition of the particles, turbulence in the chamber, the size and shape of the chamber, and particle charge [32]. Therefore, it was determined for each experiment by fitting each time series of BC data. The average particle wall-loss rate for all the experiments was -0.400±0.095 hr^{-1} (i.e., after approximately 2.5 hr the BC concentration decreased to 37% of its initial value). For experiments without enough BC to calculate a rate constant the decay of (1) sulfate from the seed particles, (2) nitrate, (3) organics after photo-oxidation or (4) total PM after photo-oxidation was used.

Using BC (or any of the other species) as a tracer for wall-loss assumes that it is internally mixed with the OA. This assumption was valid for most experiments because the size resolved data (SMPS and AMS) only showed growth of the primary mode aerosol. However, in a few experiments significant particle mass was formed from nucleation. Therefore, in these experiments it was necessary to adjust the wall-loss rate to account for the more rapid loss of smaller nucleation mode particles.

It is possible that SOA production during our experiments could cause interference with the BC measured with the aethalometer at 880 nm, thereby complicating our reliance on this instrument for determining wall-loss rates. To investigate this possibility we performed similar experiments in 2011, using a single particle soot photometer (SP2, DMT, Inc.) operating in parallel with the aethalometer. The results from the two instruments showed excellent agreement: average difference between the wall-loss rates calculated from the aethalometer and the SP2 was 4% (n=8). The two instruments operate according to entirely different principles: the aethalometer measures light adsorption caused by BC collected on a filter, whereas the SP2 measures the laser-induced incandescence of individual BC particles. The close agreement between them strongly indicates the robustness of the BC values we used to calculate wall-loss rates.

The loss of condensable organic vapors to wall-bound particles is constrained by considering two limiting cases: the first (Method #1) assumes that no organic vapors condense to wall-bound particles, and the second (Method #2) assumes that organic vapors remain in equilibrium with both wall-bound and suspended particles. The loss of organic vapors directly to the chamber walls (in distinction to their loss to wall-bound particles) is highly uncertain, and in keeping with virtually every other chamber study in the literature, we do not account for it here. If it were included, it would *increase* our estimate of SOA production.

Method #1 provides a lower bound estimate of the SOA mass production; it is equivalent to the "ω = 0" correction utilized in previous studies [14, 17]. Method #1 assumes that mass transfer resistance to the walls is much greater than to the suspended particles. This is a reasonable assumption since condensable vapors are in continuous, intimate contact with suspended particles, whereas their interaction with wall-bound particles is likely to be far less frequent. A consequence of this wall-loss assumption is that suspended and wall-bound particles may have different compositions.

Assuming no loss of vapors to the walls in Method #1, the rate at which OA mass is lost to the chamber walls is

$$\frac{d}{dt}(OA_{wall}) = OA_{sus}(-k) \quad (2)$$

where OA_{sus} is the AMS-measured (i.e., suspended) OA mass at time t and k is the negative wall-loss rate constant of black carbon [14]. The total OA in the chamber is calculated by numerically integrating equation (2) and adding the calculated OA lost to the wall to the measured OA concentration (equation (1)).

Method #2 assumes that particles lost to the walls during an experiment remain in equilibrium with the vapor phase. This case corresponds to the "ω = 1" correction [14]. The total OA mass at time t is equal to the suspended particle mass scaled by the ratio of the initial black carbon concentration to the black carbon concentration at time t

$$OA_{total,t} = OA_{sus,t} \cdot \frac{C_0}{C_t} \quad (3)$$

where C_o is the initial black carbon concentration and C_t is the measured black carbon concentration at time t. As only *suspended* OA is referenced in equation (3) the PM on the wall and in suspension has the same composition.

In experiments with low BC concentrations, the total OA estimates from Method #2 can be noisy due to their inverse dependence on BC in equation (3). For such experiments, we implemented Method #2 using the previously described exponential fit to the BC data rather than the actual BC data themselves,

$$OA_{total,t} = \frac{OA_{sus,t}}{e^{kt}} \quad (4)$$

where k is the negative wall-loss rate constant of black carbon.

Experiments of Weitkamp et al. [14] indicate that the rate of vapor uptake to particles on the walls is the same as the rate for suspended particles (Method #2), suggesting that the mass transfer resistance of organic vapors to wall-bound particles is comparable with that to suspended particles. Equation (3) and Equation (4) indicate that in Method #2 the loss of organic vapors to particles on the walls scales with the mass fraction of particles on the walls to particles in suspension. Initially (before any particle loss) there is no loss of vapors to wall but it increases as an experiment progresses. Therefore, estimates based on Method #1 and #2 diverge as more particles are lost to the wall, and the uncertainty in the observed SOA production increases as an experiment progress [33]. Given this increasing uncertainty, we imposed a 5:1 upper bound on the ratio of OA on the wall to suspended OA. This condition was binding in less than half the experiments, and when it was binding, it was typically only later in the experiment after 1.5-2.5 hours of photo-oxidation. The average and range of OA from Methods #1 and #2 is reported in the results.

Stringent regulations for new gasoline vehicles has lead to organic gas-phase emissions that approach ambient levels; thus, it is important to distinguish between SOA produced from vehicle emissions and SOA production from organic gases desorbing from the CVS, transfer line and chamber wall or from ambient organics in the dilution air. The correction for the blank SOA production and supporting experimental data are presented in detail in the section of the main text under the heading *Primary Emissions and Secondary Production from Chamber Vehicles*.

Wall-loss Rate Correction for Nucleation

Particle loss to chamber walls is a size-dependent process (smaller particles are lost faster); therefore, in experiments where a major fraction of the particle mass is created during a

nucleation event, we must modify the wall-loss rate to account for the more rapid loss of nucleation mode particles compared to BC (which is in the accumulation mode). In these cases a large fraction of the OA mass is not internally mixed with BC. Nucleation was an important factor in four of the chamber experiments. In the LEV1-1.5, LEV1-5.2, LEV2-1.2 and LEV2-2.1 experiments between 40% and 99% of the total OA mass in the chamber was in the nucleation mode within minutes of turning on the UV lights.

To illustrate the contribution of nucleation to the particle mass in the chamber, Figure S.2 and Figure S.3 present particle size distributions for experiments in which nucleation contributes negligibly and significantly to the total OA mass, respectively. Particle number and mass distributions for the LEV1-6.2 experiment at four different time points are shown in Figure S.2. This was a high emitting vehicle; the primary PM concentration in the chamber after the vehicle driving cycle (from SMPS measurements, assuming unit density) was approximately 13 $\mu g\ m^{-3}$. While nucleation does occur in this experiment—as evidenced by the large peak at about 20 nm in the number size distribution—only 3% of the particle mass is in the nucleation mode ten minutes after nucleation. Most of the secondary mass condenses onto accumulation mode particles. Nevertheless, the growth of the nucleation mode particles toward the primary mode still results in a shift in the mass distribution to smaller sizes than before nucleation, but it is slight and should not impact wall-loss estimate from the BC data significantly.

In contrast, Figure S.3 presents the size distributions for the LEV1-5 vehicle, a low-emitting vehicle. The primary PM concentration in the chamber after the vehicle driving cycle (from SMPS measurements, assuming unit density) was approximately 2 $\mu g\ m^{-3}$. In Figure S.3, the nucleation peak at 20 nm, formed -0.19 hr after the UV lights were turned on, completely dominates both the two primary particle number concentrations (the pre-nucleation number concentrations lie very close to the x-axis and can't be readily discerned in the figure because of the size of the nucleation peak) and the two primary particle mass concentrations. In this experiment, the nucleation mode contributed 63% of the total particle mass within 0.19 hr after lights on. The mass distribution for the LEV1-5 vehicle on the right side of Figure S.3 shows a major shift in the mass median diameter from about 190 nm for the primary PM emissions at t=0 h to about 32 nm at t=0.19 h occurs. Because of the dominant nucleation mode in this experiment, the wall-loss rate of BC in the 190 nm primary mode is not a good model for the nucleated particles; if the BC wall-loss rate were used to estimate the loss of the nucleated organics, we would substantially underpredict the actual SOA production.

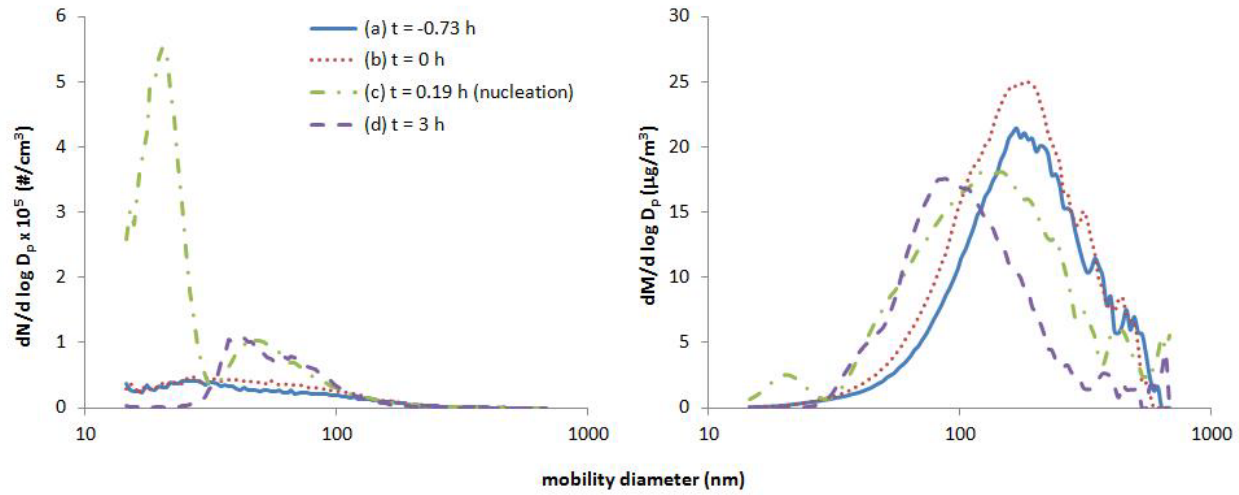

Figure S.2 Particle number (left) and mass (right) distributions for the LEV1-6.2 experiment (a) immediately after injection of emissions into the chamber ceased, (b) just before lights on, (c) at the beginning of a small nucleation event about 15 minutes after lights were turned on, and (d) 3 hours after lights were turned on.

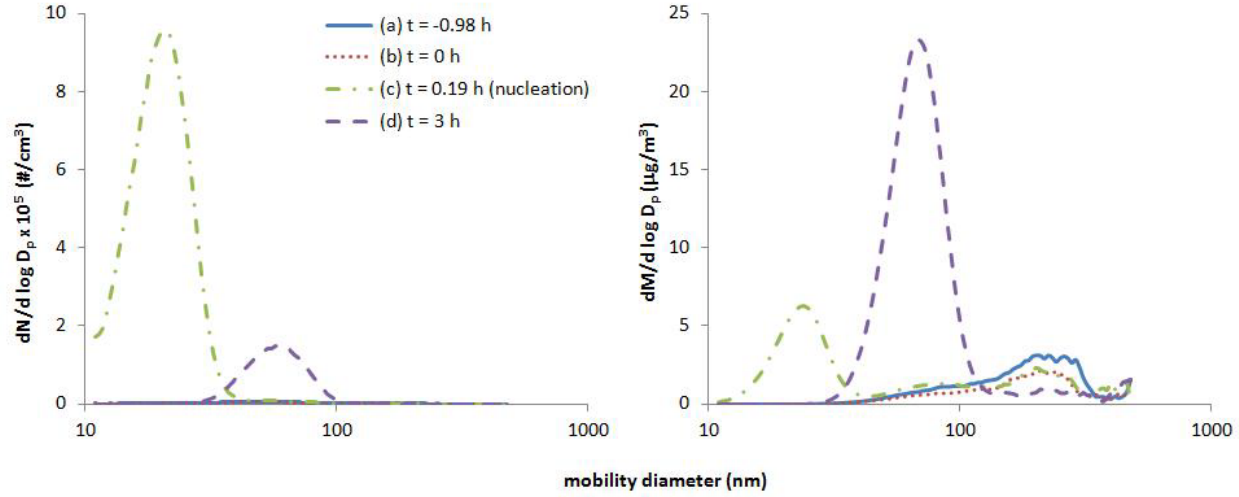

Figure S.3 Particle number (left) and mass (right) distributions for the LEV1-5 vehicle (a) immediately after injection of emissions into the chamber ceased, (b) just before lights on, (c) at the beginning of a very large nucleation event about 15 minutes after lights were turned on, and (d) 3 hours after lights were turned on.

In the four experiments where the nucleation mode contributes more than 25% of the suspended aerosol mass, we corrected the wall-loss rate, *k*, for particle size. Our approach assumes that wall-loss of nucleation mode particles is governed by Brownian diffusion. Crump and Seinfeld derived an expression for the size-dependent wall-loss rate for particles in a spherical chamber of radius *R*

$$k_w(D_p) = \frac{6\sqrt{k_e D}}{\pi R} D_1\left(\frac{\pi v_s}{2\sqrt{k_e D}}\right) + \frac{v_s}{4R/3} \qquad (1)$$

where D is the Brownian diffusivity for particles of diameter D_p, k_e (units of time^{-1}) is a function of the turbulent kinetic energy in the chamber, v_s is the gravitational settling velocity of the particle (negligible for nucleation mode particles) and $D_1(\ldots)$ is the Debye function [48].

Equation (1) indicates that the wall-loss rate scales with the square root of diffusivity, which in turn, is inversely proportional to particle diameter [32]. We therefore scale the wall-loss rate of the nucleation mode, k_{nuc}, using the wall-loss rate of the primary mode, k, and the diameters of the nucleation mode, d_{nuc}, and the primary mode, d

$$k_{nuc} = k \cdot \sqrt{\frac{d}{d_{nuc}}} \qquad (2)$$

Figure S.4 illustrates the impact of correcting for the more rapid loss of nucleation mode particles on the organic aerosol estimates. There is ≈20% increase in OA when the nucleation correction is employed with wall-loss correction method #1 and about a ≈50% increase for Method #2. The relative changes shown in Figure S.4 are comparable for the other experiments with a significant nucleation mode.

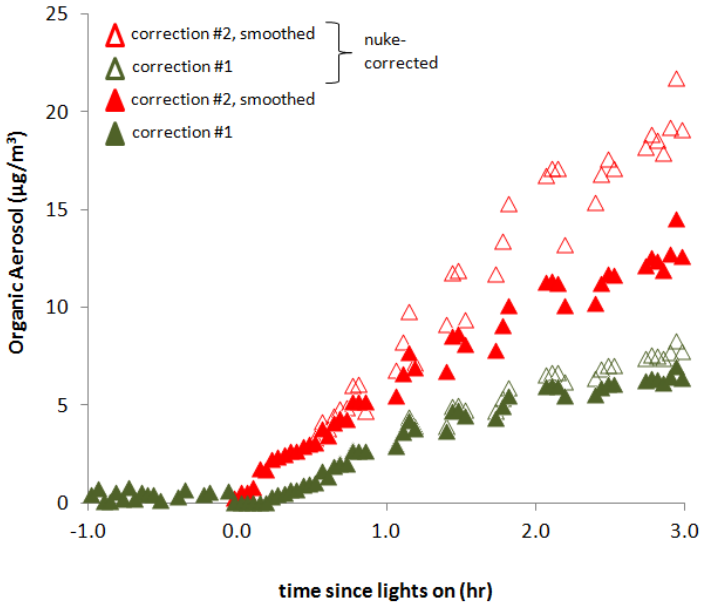

Figure S.4 Wall-loss-corrected OA for the LEV2-2.1 vehicle with and without nucleation correction.

AMS Corrections: Comparison with SMPS Measurements

Theoretically, the sum of the PM mass from the non-refractory components (measured by the AMS) and BC (measured by the aethalometer) should be equal to the mass calculated from the SMPS size distributions. These three sets of data provide two independent methods of calculating PM, but each method has limitations, complicating the comparison.

First, the SMPS measures particle mobility diameter, while the AMS measures mass. To convert SMPS measurements to mass one must assume a particle shape and density. We assume that particles are spherical with average density of 1 g/cm^3. However, fractal-like particles will cause the SMPS to overestimate the spherical equivalent diameter and therefore overestimate particle mass. While commonly made, the unit density [49] and sphericity [50, 51] assumptions have both been shown to not always be valid for aerosol with high EC (e.g., diesel

emissions). After SOA production begins the sphericity assumption improves as the organics coat the primary particles, making them more spherical [52].

Second, the mass measured by the AMS will be less than the true PM mass due to three artifacts whose product is referred to as the AMS collection efficiency:

$$C_e(d_{va}) = E_L(d_{va}) \times E_S(d_{va}) \times E_B(d_{va}) \quad (3)$$

where d_{va} is the particle vacuum aerodynamic diameter. The transmission efficiency, E_L, of the AMS's aerodynamic lens is size-dependent with a detection window that falls off above 600 nm and below 120 nm [53]. E_S is the striking efficiency, which refers to the tendency of non-spherical particles to miss the AMS's vaporizer as they are conveyed from the time-of-flight chamber. E_B quantifies the fraction of particles that bounce off of the AMS's vaporizer before they are measured. Bounce is a function of particle phase (solid/liquid), particle acidity and ambient RH, among other factors. For an internally mixed aerosol (which is likely in these experiments once SOA forms), the same collection efficiency should be used for all chemical species [54]. Losses due to striking efficiency appear to be less than 20% for ambient particles [55].

For the four experiments with substantial nucleation, a large fraction of the particle mass was in the 10 nm < d_{va} < 30 nm range and, therefore, was not detected by the AMS. Thus, the calculated OA production in these experiments is likely to deviate from the true value due to (1) the increased wall-loss rates experienced by nucleation mode particles, (2) the reduced AMS transmission efficiency of particles below the detection window and (3) other collection efficiency effects (i.e., E_S and E_B).

In addition to the four experiments with major nucleation events, there were other experiments with somewhat larger mass median particle sizes (80 nm < d_{va} < 120 nm); it was not necessary to correct the wall-loss rates for nucleation in these experiments, but the collection efficiency effects were still important. In particular, some fraction of the particles in such experiments is not transmitted through the lens due to the AMS's size-detection limitations. Figure S. 5 presents an example of such an experiment. It shows that the sum of the non-refractory components and BC for the LEV1-6.2 experiment are approximately a factor of two lower than the mass calculated from the SMPS size distributions (assuming spherical particles and density of 1 g cm^{-3}). As previously discussed, while there is nucleation in this experiment Figure S.2, it has only a minor impact on the mass distribution—unlike the large nucleation effect found in experiments with behavior as described in Figure S.3. Nevertheless, as this experiment demonstrates, the AMS detection window artifact can be important in experiments even when the nucleation event is small and does not have a major impact on the overall mass distribution (and thus the wall-loss rate).

We assume that the discrepancy between the sum of the speciated masses and the SMPS-derived mass shown in Figure S. 5 is primarily due to E_L. While it is possible that particle bounce and/or striking efficiency may be responsible for some of the discrepancy, we cannot readily deconvolve the three components of the collection efficiency, and, furthermore, even if we could, it is not obvious that correcting for them would require a different approach than the simplified approach we describe next.

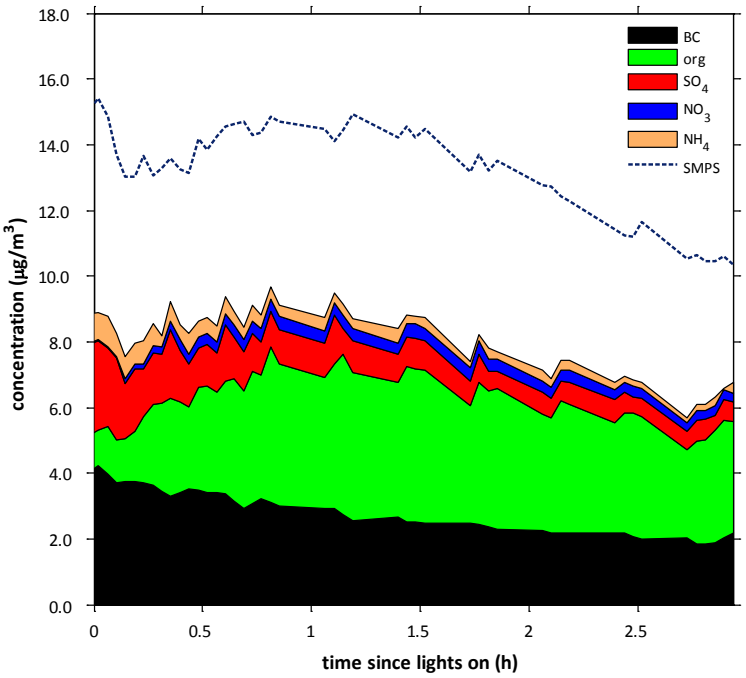

Figure S.5 Comparison of the sum of BC (measured by the aethalometer), organics, sulfate, nitrate and ammonium (measured by the AMS) against the total particle mass measured by the SMPS for the LEV1-6.2 experiment. Data are not wall-loss corrected.

For those experiments with the AMS+BC vs. SMPS discrepancy, we assume that the difference in mass has the same chemical composition as the speciated components. We then calculate a scaling factor, $AMS_{s.f.}$, that increases the sizes of the four colored wedges in Figure S. 5 proportionally such that their sum closes the gap with the SMPS measurement (dashed line). The scaling factor is

$$AMS_{s.f.} = \frac{C_{SMPS} - C_{BC}}{C_{org} + C_{SO_4} + C_{NO_3} + C_{NH_4}} \quad (4)$$

where C_{SMPS} is the total particle concentration measured by the SMPS, C_{BC} is the black carbon concentration measured by the aethalometer, C_{org}, C_{SO_4}, C_{NO_3}, and C_{NH_4} are the concentrations of organics, sulfate, nitrate and ammonium measured by the AMS. The values for $AMS_{s.f.}$ were calculated for each time step after nucleation, excluding the times when the aerosol passed through the thermodenuder, and then these values were averaged over the three hour UV exposure period. The $AMS_{s.f.}$ was used to scale the AMS data for the LEV1-5.2, LEV1-6.1, LEV1-6.2, LEV2-1.6, LEV2-2.1 and LEV2-4.2 experiments. In these experiments the average $AMS_{s.f.}$ ranged between 1.13 and 2.01, and the coefficient of variation within each experiment was between 7% and 18%. The $AMS_{s.f.}$ was not used to scale the data from other experiments either because the larger median particle size didn't warrant it or because the $AMS_{s.f.}$ was too uncertain (i.e., the COV was greater than 20%).

Table S.5 NMOGs as discussed in Figure 3, their OH reaction rates and the SOA yield cases in which they are included (Figure 7).

	Compound	speciated SOA precursor (Fig. 3)?	included only in lower SOA yield estimate (Fig. 7)?	OH rxn rate (cm^3-$molec^{-1}$ sec^{-1})
Hydrocarbons	ethane	no	no	2.48E-13
	ethene	no	no	8.52E-12
	propane	no	no	1.09E-12
	propene	no	no	2.63E-11
	methylpropane	no	no	2.12E-12
	ethyne	no	no	8.15E-13
	n-butane	no	no	2.36E-12
	1,2-propadiene	no	no	9.82E-12
	trans-2-butene	no	no	6.40E-11
	1-butene	no	no	3.14E-11
	2-methyl-2-butene	no	no	8.69E-11
	cis-2-butene	no	no	5.64E-11
	2,2-dimethylpropane	no	no	6.69E-13
	2-methylbutane	no	no	3.60E-12
	1-propyne	no	no	7.14E-12
	1,2-butadiene	no	no	2.60E-11
	1,3-butadiene	no	no	6.66E-11
	trans-2-pentene	no	no	6.70E-11
	2-methylpropene	no	no	5.14E-11
	1-pentene	no	no	3.14E-11
	2-methyl-1-butene	no	no	6.10E-11
	cis-2-pentene	no	no	6.50E-11
	1-buten-3-yne	no	no	4.01E-11
	2-butyne	no	no	2.73E-11
	1-butyne	no	no	8.10E-12
	1,3-butadiyne	no	no	1.82E-11
	3-methyl-1-butene	no	no	2.86E-11
	n-pentane	no	no	3.80E-12
	2-methyl-1,3-butadiene	no	no	1.00E-10
	3,3-dimethyl-1-butene	no	no	2.80E-11
	trans-1,3-pentadiene	no	no	1.60E-12
	2,2-dimethylbutane	no	no	2.23E-12
	cyclopentene	no	no	6.70E-11
	4-methyl-1-pentene	no	no	3.02E-11
	3-methyl-1-pentene	no	no	3.02E-11
	cyclopentane	no	no	4.97E-12
	2,3-dimethylbutane	no	no	5.78E-12
	2,3-dimethyl-1-butene	no	no	5.38E-11
	methyl-tert-butyl-ether	no	no	2.26E-12
	4-methyl-cis-2-pentene	no	no	5.88E-11
	2-methylpentane	no	no	5.45E-12
	4-methyl-trans-2-pentene	no	no	6.64E-11
	3-methylpentane	no	no	5.73E-12
	1-hexene	no	no	3.70E-11
	2-methyl-1-pentene	no	no	5.40E-11
	n-hexane	no	no	6.97E+12
	trans-3-hexene	no	no	6.62E-11
	cis-3-hexene	no	no	5.86E-11
	trans-2-hexene	no	no	6.66E-11

	Compound	speciated SOA precursor (Fig. 3)?	included only in lower SOA yield estimate (Fig. 7)?	OH rxn rate (cm^3-$molec^{-1}$ sec^{-1})
Hydrocarbons	2-methyl-2-pentene	no	no	8.90E-11
	3-methyl-trans-2-pentene	no	no	8.83E-11
	3-methylcyclopentene	no	no	5.97E-11
	cis-2-hexene	no	no	5.90E-11
	3-methyl-cis-2-pentene	no	no	8.83E-11
	1-ethyl-tert-butyl-ether	no	no	7.60E-12
	2,2-dimethylpentane	no	no	3.23E-12
	methylcyclopentane	no	no	5.66E-12
	2,4-dimethylpentane	no	no	4.77E-12
	2,2,3-trimethylbutane	no	no	3.81E-12
	3,4-dimethyl-1-pentene	no	no	3.16E-11
	2,4-dimethyl-1-pentene	no	no	5.54E-11
	1-methylcyclopentene	no	no	8.94E-11
	benzene	yes	no	1.22E-12
	3-methyl-1-hexene	no	no	3.16E-11
	3,3-dimethylpentane	no	no	2.97E-12
	2,4-dimethyl-2-pentene	no	no	8.94E-11
	cyclohexane	no	no	6.97E-12
	2-methyl-trans-3-hexene	no	no	6.74E-11
	4-methyl-trans-2-hexene	no	no	6.80E-11
	2-methylhexane	no	no	6.86E-12
	2,3-dimethylpentane	no	no	7.14E-12
	cyclohexene	no	no	6.77E-11
	3-methylhexane	no	no	7.15E-12
	trans-1,3-dimethylcyclopentane	no	no	6.80E-12
	cis-1,3-dimethylcyclopentane	no	no	6.80E-12
	3-ethylpentane	no	no	7.56E-12
	trans-1,2-dimethylcyclopentane	no	no	6.80E-12
	2,2,4-trimethylpentane	no	no	3.34E-12
	1-heptene	no	no	4.00E-11
	3-methyl-trans-3-hexene	no	no	8.92E-11
	trans-3-heptene	no	no	6.76E-11
	n-heptane	no	no	6.76E-12
	2,4,4-trimethyl-1-pentene	no	no	5.32E-11
	2-methyl-2-hexene	no	no	8.96E-11
	trans-2-heptene	no	no	6.80E-11
	3-ethyl-2-pentene	no	no	8.92E-11
	3-methyl-cis-2-hexene	no	no	8.96E-11
	2,3-dimethyl-2-pentene	no	no	1.03E-10
	cis-2-heptene	no	no	6.04E-11
	methylcyclohexane	no	no	9.64E-12
	2,2-dimethylhexane	no	no	4.64E-12
	2,4,4-trimethyl-2-pentene	no	no	8.77E-11
	ethylcyclopentane	no	no	7.24E-12
	2,5-dimethylhexane	no	no	8.27E-12
	2,4-dimethylhexane	no	no	8.55E-12
	1,2,4-trimethylcyclopentane	no	no	7.95E-12
	3,3-dimethylhexane	no	no	4.38E-12
	1a,2a,3b-trimethylcyclopentane	no	no	7.95E-12
	2,3,4-trimethylpentane	no	no	6.60E-12
	toluene	yes	no	5.63E-12
	2,3,3-trimethylpentane	no	no	4.37E-12

	Compound	speciated SOA precursor (Fig. 3)?	included only in lower SOA yield estimate (Fig. 7)?	OH rxn rate (cm^3-$molec^{-1}$ sec^{-1})
Hydrocarbons	2,3-dimethylhexane	no	no	8.55E-12
	2-methylheptane	no	no	4.77E-12
	4-methylheptane	no	no	8.56E-12
	3,4-dimethylhexane	no	no	8.84E-12
	3-methylheptane	no	no	8.56E-12
	cis-1,2-dimethylcyclohexane	no	no	1.19E-11
	trans-1,4-dimethylcyclohexane	no	no	1.19E-11
	2,2,5-trimethylhexane	yes	no	6.05E-12
	trans-1-methyl-3-ethylcyclopentane	no	no	8.39E-12
	cis-1-methyl-3-ethylcyclopentane	no	no	8.39E-12
	1-octene	no	no	3.30E-11
	2,2,4-trimethylhexane	yes	no	6.33E-12
	trans-4-octene	no	no	6.90E-11
	n-octane	no	no	8.11E-12
	trans-2-octene	no	no	6.94E-11
	trans-1,3-dimethylcyclohexane	no	no	1.19E-11
	2,4,4-trimethylhexane	yes	no	5.78E-12
	cis-2-octene	no	no	6.18E-11
	2,3,5-trimethylhexane	yes	no	9.96E-12
	2,4-dimethylheptane	yes	no	9.97E-12
	cis-1,3-dimethylcyclohexane	no	no	1.19E-11
	2,6-dimethylheptane	yes	no	9.68E-12
	ethylcyclohexane	no	no	1.20E-11
	3,5-dimethylheptane	yes	no	1.02E-11
	ethylbenzene	yes	no	7.00E-12
	1,3,5-trimethylcyclohexane	yes	no	1.35E-11
	2,3-dimethylheptane	yes	no	9.97E-12
	m-xylene	yes	no	2.31E-11
	p-xylene	yes	no	1.43E-11
	4-methyloctane	yes	no	9.97E-12
	2-methyloctane	yes	no	9.69E-12
	3-methyloctane	yes	no	9.97E-12
	styrene	yes	no	5.80E-11
	o-xylene	yes	no	1.36E-11
	2,2,4-trimethylheptane	yes	no	7.75E-12
	1-methyl-4-ethylcyclohexane	yes	no	1.37E-11
	2,2,5-trimethylheptane	yes	no	7.75E-12
	1-nonene	yes	no	3.44E-11
	n-nonane	yes	no	9.70E-12
	3,3-dimethyloctane	yes	no	7.21E-12
	(1-methylethyl)benzene	yes	no	6.90E-12
	2,3-dimethyloctane	yes	no	1.14E-11
	2,2-dimethyloctane	yes	no	7.47E-12
	2,5-dimethyloctane	yes	no	1.14E-11
	2,4-dimethyloctane	yes	no	1.14E-12
	2,6-dimethyloctane	yes	no	1.14E-13
	n-propylbenzene	yes	no	5.80E-12
	1-methyl-3-ethylbenzene	yes	no	1.39E-11
	1-methyl-4-ethylbenzene	yes	no	7.44E-12
	1,3,5-trimethylbenzene	yes	no	5.67E-11
	2-methylnonane	yes	no	1.11E-11
	1-methyl-2-ethylbenzene	yes	no	7.44E-12

	Compound	speciated SOA precursor (Fig. 3)?	included only in lower SOA yield estimate (Fig. 7)?	OH rxn rate (cm^3-$molec^{-1}$ sec^{-1})
Hydrocarbons	1,2,4-trimethylbenzene	yes	no	3.25E-11
	(2-methylpropyl)benzene	yes	no	8.71E-12
	(1-methylpropyl)benzene	yes	no	8.50E-12
	n-decane	yes	no	1.10E-11
	1-methyl-3-(1-methylethyl)benzene	yes	no	1.45E-11
	1,2,3-trimethylbenzene	yes	no	3.27E-11
	1-methyl-4-(1-methylethyl)benzene	yes	no	8.54E-12
	indan	yes	no	8.28E-12
	1-methyl-2-(1-methylethyl)benzene	yes	no	8.54E-12
	1,3-diethylbenzene	yes	no	3.25E-11
	1-methyl-3-n-propylbenzene	yes	no	1.52E-11
	1,4-diethylbenzene	yes	no	3.25E-11
	1-methyl-4-n-propylbenzene	yes	no	8.80E-12
	1,3-dimethyl-5-ethylbenzene	yes	no	3.44E-11
	1,2-diethylbenzene	yes	no	5.80E-12
	1-methyl-2-n-propylbenzene	yes	no	8.80E-12
	1,4-dimethyl-2-ethylbenzene	yes	no	1.69E-11
	1,3-dimethyl-4-ethylbenzene	yes	no	1.76E-11
	1,2-dimethyl-4-ethylbenzene	yes	no	1.69E-11
	1,3-dimethyl-2-ethylbenzene	yes	no	1.76E-11
	n-undecane	yes	no	1.25E-11
	1,2-dimethyl-3-ethylbenzene	yes	no	1.69E-11
	1,2,4,5-tetramethylbenzene	yes	no	3.25E-11
	1,2,3,5-tetramethylbenzene	yes	no	4.31E-11
	1-(dimethylethyl)-2-methylbenzene	yes	no	6.74E-12
	5-methylindan	yes	no	1.79E-11
	4-methylindan	yes	no	1.79E-11
	1-ethyl-2-n-propylbenzene	yes	no	9.47E-12
	2-methylindan	yes	no	9.42E-12
	1,2,3,4-tetramethylbenzene	yes	no	2.05E-11
	n-pentylbenzene	yes	no	1.01E-11
	1-methyl-2-n-butylbenzene	yes	no	1.02E-11
	naphthalene	yes	no	2.30E-11
	1-(dimethylethyl)-3,5-dimethylbenzene	yes	no	3.01E-11
	1,3-di-n-propylbenzene	yes	no	1.08E-11
	n-dodecane	yes	no	1.32E-11
Carbonyls	formaldehyde	no	no	9.37E-12
	acetaldehyde	no	no	1.50E-11
	acrolein	no	no	2.58E-11
	acetone	no	no	1.70E-13
	propionaldehyde	no	no	2.20E-11
	crotonaldehyde	no	no	3.62E-11
	methacrolein	no	no	2.90E-11
	MEK	no	no	1.33E-12
	butyraldehyde	no	no	2.40E-11
	benzaldehyde	yes	no	1.20E-11
	valeraldehyde	no	no	2.74E-11
	m-tolualdehyde	yes	no	1.70E-11
	hexanal	no	no	3.00E-11
Other	unspeciated NMOG	no	yes	2.00E-11
	SVOC/IVOC	yes	yes	3.00E-11

Table S.6. Emission factors measured in the CVS and SOA production factors for all chamber experiments.

	test date	CARB test ID	expt ID	model year	UC driving cycle	NMOG (g/kg)	CO (g/kg)	NOx (g/kg)	CVS POA (mg/kg)	EC (mg/kg)	SOA, OH=5x10^6 (mg/kg)
Pre-LEV	2/14/12	1032442	PreLEV-1.1	1987	Cold	8.82	209.46	8.79	54.1	35.9	26.9
	2/10/12	1032440	PreLEV-2.1	1988	Cold	34.98	332.34	19.64	136.3	44.4	108.4
	2/13/12	1032444	PreLEV-2.2		Cold	31.41	328.25	19.48	102.4	29.2	89.6
	1/31/12	1032303	PreLEV-3.2	1990	Cold	5.62	72.07	8.16	57.8	2.4	46.7
	2/1/12	1032389	PreLEV-3.3		Cold	5.36	73.14	8.34	48.7	3.1	70.2
	2/8/12	1032426	PreLEV-3.4		Hot	2.68	49.56	5.44	0.5	2.4	n/a
LEV I	5/26/10	1027859	LEV1-1.5	1996	Cold	2.35	19.83	4.44	3.4	0.8	10.1
	1/17/12	1032302	LEV1-2.1	1997	Cold	1.28	17.90	2.34	0.1	1.9	n/a
	1/18/12	1032304	LEV1-2.2		Cold	1.49	22.57	2.39	0.8	3.0	43.7
	2/15/12	1032473	LEV1-2.3		Hot	0.23	9.97	1.25	4.1	4.0	22.3
	1/25/12	1032346	LEV1-3.2	1998	Cold	1.13	24.63	2.07	0.4	3.3	39.8
	1/26/12	1032362	LEV1-3.4		Cold	1.20	28.36	2.30	0.2	1.4	56.1
	2/6/12	1032393	LEV1-4.1	1999	Cold	0.95	45.32	3.63	2.3	4.0	35.2
	6/3/10	1027904	LEV1-5.2	2000	Cold	1.61	14.77	2.05	26.1	3.5	35.6
	5/28/10	1027881	LEV1-6.1	2003	Cold	17.82	162.62	21.16	101.9	86.7	30.3
	6/1/10	1027917	LEV1-6.2		Cold	15.02	157.54	20.16	106.2	122.2	131.4
	6/2/10	1027918	LEV1-6.3		Cold	15.47	155.48	21.97	88.8	51.6	n/a
LEV II	5/27/10	1027865	LEV2-1.2	2007	Cold	0.60	17.94	0.40	4.6	12.0	35.8
	6/9/10	1027967	LEV2-1.6		Cold	0.53	21.16	0.45	2.2	12.5	26.3
	6/15/10	1028022	LEV2-2.1	2008	Cold	0.67	7.78	0.57	4.8	21.1	10.4
	1/12/12	1032268	LEV2-3.1	2008	Cold	0.42	7.12	0.30	0.0	0.0	8.8
	1/13/12	1032283	LEV2-3.2		Cold	0.50	9.13	0.34	0.3	12.8	31.8
	1/27/12	1032360	LEV2-3.3		Hot	0.08	2.10	0.16	-0.5	10.7	6.3
	1/30/12	1032359	LEV2-3.4		Hot	0.20	1.24	0.23	0.0	13.6	1.6
	6/10/10	1027971	LEV2-4.2	2010	Cold	0.40	6.33	0.08	2.4	33.2	17.4
	1/23/12	1032342	LEV2-5.1	2011	Cold	0.41	21.44	0.56	4.1	32.1	54.6
	1/24/12	1032351	LEV2-5.2		Cold	0.51	14.97	0.63	1.3	35.2	24.9
	1/19/12	1032309	LEV2-6.2	2011	Cold	0.59	11.99	0.21	-0.4	2.4	4.3
	1/20/12	1032321	LEV2-6.3		Cold	0.74	9.20	0.15	0.3	1.1	2.0

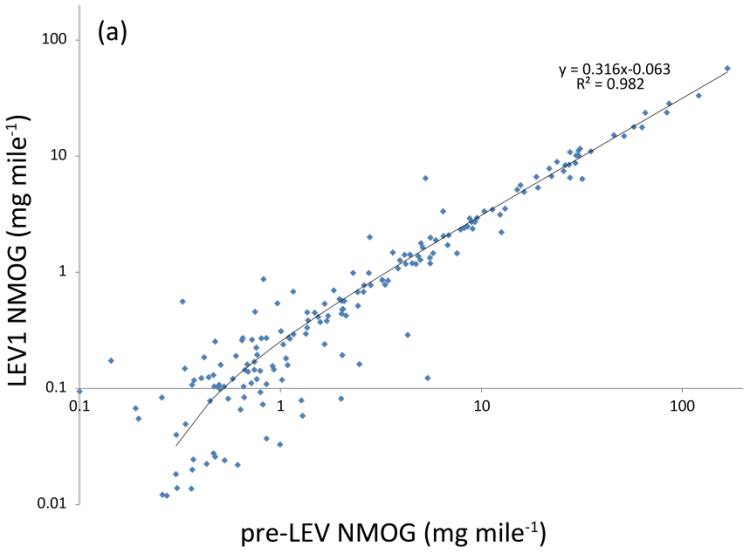
(a)
y = 0.316x-0.063
R² = 0.982
LEV1 NMOG (mg mile-1)
pre-LEV NMOG (mg mile-1)
100
10
1
0.1
0.01
0.1
1
10
100

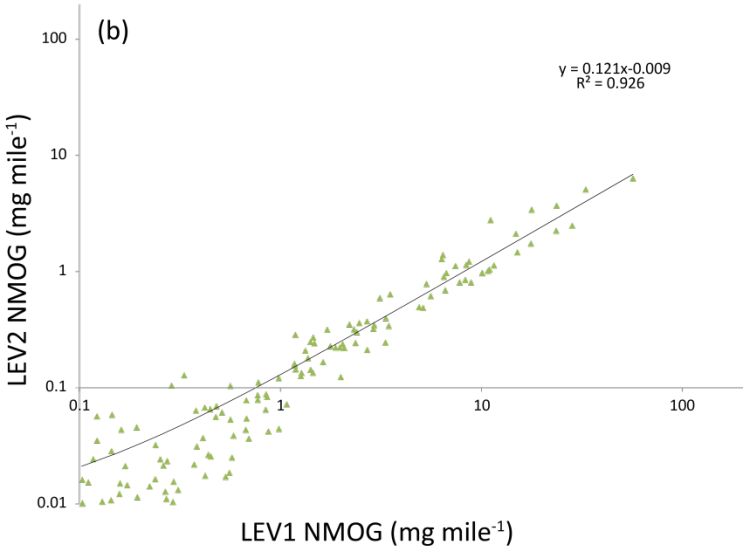
(b)
y = 0.121x-0.009
R² = 0.926
LEV2 NMOG (mg mile-1)
LEV1 NMOG (mg mile-1)
100
10
1
0.1
0.01
0.1
1
10
100

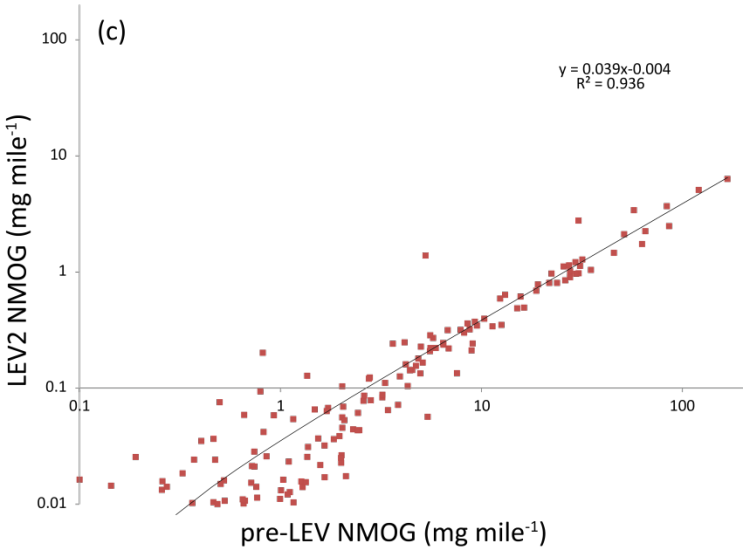
(c)
y = 0.039x-0.004
R² = 0.936
LEV2 NMOG (mg mile-1)
pre-LEV NMOG (mg mile-1)
100
10
1
0.1
0.01
0.1
1
10
100

Figure S.6. Log-log plots of individual NMOG species detected by the GC. Points above (below) the trendlines indicate species that were reduced less (more) than the majority of the other species. The lack of significant outliers suggests that the relatively small reduction in SOA production for newer LEV2 vehicles is due to unspeciated SOA precursors rather than those identified by the GC.